Compulsivity and impulsivity traits linked to attenuated developmental fronto-striatal myelination trajectories

Gabriel Ziegler[1,2,3,4,*], Tobias U. Hauser[1,2,*], Michael Moutoussis[1,2], Edward T. Bullmore[5,6,7,8], Ian M. Goodyer[5,6], Peter Fonagy[9], Peter B. Jones[5,6], NSPN Consortium[10], Ulman Lindenberger[1,11] & Raymond J. Dolan[1,2]

[1] Max Planck University College London Centre for Computational Psychiatry and Ageing Research, London, United Kingdom, and Berlin (Dahlem), Germany
[2] Wellcome Centre for Human Neuroimaging, University College London, London, United Kingdom
[3] Institute of Cognitive Neurology and Dementia Research, Otto-von-Guericke-University Magdeburg, Magdeburg, Germany
[4] German Center for Neurodegenerative Diseases (DZNE), Magdeburg, Germany
[5] Department of Psychiatry, University of Cambridge, Cambridge, United Kingdom
[6] Cambridgeshire and Peterborough National Health Service Foundation Trust, Cambridge, United Kingdom
[7] Medical Research Council/Wellcome Trust Behavioural and Clinical Neuroscience Institute, University of Cambridge, Cambridge, United Kingdom
[8] ImmunoPsychiatry, GlaxoSmithKline Research and Development, Stevenage, United Kingdom
[9] Research Department of Clinical, Educational and Health Psychology, University College London, London, United Kingdom
[10] A full list of authors can be found in the Supplementary Note
[11] Center for Lifespan Psychology, Max Planck Institute for Human Development, Berlin, Germany
* These authors contributed equally to this work

Correspondence
Tobias U. Hauser
Max Planck UCL Centre for Computational Psychiatry and Ageing Research
University College London
10-12 Russell Square
London WC1B 5EH
United Kingdom
Phone: +44 / 207 679 5264
Email: t.hauser@ucl.ac.uk

Gabriel Ziegler
Institute of Cognitive Neurology and Dementia Research
German Center for Neurodegenerative Diseases (DZNE)
Otto-von-Guericke-University Magdeburg
Leipziger Str. 44
39120 Magdeburg
Germany
Phone: +49 / 391 67 250 54
Email: gabriel.ziegler@dzne.de

Abstract

The transition from adolescence into adulthood is a period when ongoing brain development coincides with a substantially increased risk of psychiatric disorders. The developmental brain changes accounting for this emergent psychiatric symptomatology remain obscure. Capitalising on a unique longitudinal dataset that includes *in-vivo* myelin-sensitive magnetization transfer (MT) MRI, we show that this developmental period is characterised by brain-wide growth in MT, within both gray matter and adjacent juxta-cortical white matter. In this healthy population the expression of common developmental traits, namely compulsivity and impulsivity, is tied to a reduced growth of these MT trajectories in fronto-striatal regions. This reduction is most marked in dorsomedial and dorsolateral prefrontal regions for compulsivity, and in lateral and medial prefrontal regions for impulsivity. The findings highlight that psychiatric traits of compulsivity and impulsivity are linked to regionally specific reduction in myelin-related growth in late adolescent brain development.

Introduction

Structural brain development extends into adulthood, particularly so in regions that mediate higher cognition such as prefrontal cortex[1]. A canonical view is that this maturation is characterised by regional shrinkage in gray matter (GM) coupled to an expansion of white matter (WM)[2]. However, the underlying microstructural processes remain obscure. Two candidate mechanisms are proposed[3], namely synaptic loss (pruning) that reduces supernumerary connections, and an increase in myelination that serves to enhance communication efficiency. Both accounts receive a degree of support from cross-sectional and ex-vivo studies[4–7]. What is also known is that there are substantial inter-individual differences in these growth trajectories[8], with the most marked changes occurring within an age window where an emergence of psychiatric illness is increasingly common[9,10]. This raises a possibility that this enhanced psychiatric risk is tied to altered maturational brain trajectories during this critical developmental period[11,12].

Compulsivity and impulsivity are two important symptom dimensions in psychiatry[13] that also show substantial variation in expression within a healthy population (Supplementary Fig. 1a-f). At the extreme these axes can manifest as obsessive-compulsive disorder (OCD) and attention-deficit/hyperactivity disorder (ADHD) respectively. Macrostructural and cross-sectional studies suggest a link to changes in fronto-striatal regions[13–16], but leave unanswered the question of whether compulsivity and impulsivity reflect consequences of altered developmental microstructural processes.

Here we used semi-quantitative structural MRI[17] to investigate the microstructural brain development during a transition into adulthood, specifically asking whether individual variability in these developmental brain trajectories is linked to the expression of compulsive and impulsive traits. We used a novel magnetic transfer saturation (MT) imaging protocol to provide an *in-vivo* marker for macromolecules, in particular myelin[18,19]. Importantly, MT

saturation has been shown to be a more direct reflection of myelin compared to other imaging protocols, such as magnetization transfer ratio[20,21]. It is also sensitive to developmental effects[7]. This renders it ideal for tracking patterns of brain maturation in longitudinal studies involving repeated scanning of participants, a crucial necessity for a full characterisation of development[22]. Using such a protocol, we show that during late adolescence and early adulthood cingulate cortex expresses the greatest myelin-related growth, both within gray and adjacent white matter. Individual differences in compulsivity are reflected in a reduced rate of this growth particularly within dorsomedial and dorsolateral frontal regions. This contrasted with impulsivity, which was associated with reduced myelin-related growth in lateral and medial prefrontal cortex. Our results suggest that within an otherwise healthy population heterogeneity, compulsivity and impulsivity traits reflect regionally distinct differential growth in myelin growth trajectories.

Results

Ongoing myelin-related growth at the edge of adulthood

To assess developmental trajectories of myelin-sensitive MT we exploited an accelerated longitudinal design that included repeated scanning in 288 (149 female) adolescents and young adults aged 14–24 years, up to three times in all, with an average follow-up time of 1.3±0.32 years (mean±SD) (1 scan: N=100, 2 scans: N=167, 3 scans: N=21). The sample was gender balanced and comprised of otherwise healthy subjects (excluding self-reported illness a priori to avoid illness-related confounds, such as medication effects) who were selected to be approximately representative of the population (cf online methods for details).

Examining individual, ongoing maturation using whole-brain voxel-based quantification analyses (Supplementary Fig. 2a-b) in gray matter revealed a brain-wide increase in myelin-related MT, with a strong emphasis within cingulate, prefrontal and temporo-parietal areas (Fig. 1a, $p<.05$ false-discovery rate [FDR] peak corrected; merging cross-sectional and longitudinal effects, mean change in GM (±SD): 0.58±0.19% per year; max z-value voxel [$z=6.78$, $p<.002$ FDR] in right angular gyrus [MNI: 51 -46 44]: 0.98% per year; cf. Supplementary Table 1 for parametric and non-parametric results; separate cross-sectional and longitudinal effects shown in Supplementary Fig. 3a-b). These developmental changes were accompanied by increased MT in adjacent (juxta-cortical) superficial white matter with a similar topography to that seen in gray matter (Fig. 1b, mean change: 0.47±0.18% per year; max z-value voxel [$z=6.18$, $p<.004$ FDR] in posterior cingulate [5 -58 56] with 0.89% per year; cf. Supplementary Table 1), consistent with the idea that connections within gray and white matter are myelinated in concert (correlation between neighbouring gray-/white-matter voxels: Pearson $r=0.25$, permutation $p<0.001$; cf. online methods). Similar, albeit less pronounced, microstructural maturation was observed in

subcortical gray matter nuclei including amygdala, ventral and posterior striatum, pallidum and dorsal thalamus (Fig. 1c, mean change: 0.29±0.06% per year; max z-value voxel [z=5.12, p<.004 FDR] in amygdala [25 4 -23] with 0.5% per year). These findings highlight that myelin-related MT development in both cortical and subcortical areas is a marked feature of a transition from adolescence into adulthood, and conforms to a pattern that is suggestive of involvement of both local and inter-regional fibre projections.

Association between macro- and microstructural development

The observed developmental expansion of myelin-sensitive MT expressed overlapping topographies with macrostructural gray matter shrinkage (with the exception of hippocampus) and white matter expansion (Fig. 2a; Supplementary Fig. 4a-c and Supplementary Table 2 for macrostructural results). This raises a question as to how precisely macrostructural volume change relates to development of our myelin marker MT. A positive association in white matter volume (Fig. 2b-c; mean±SD: r=0.09±0.05, t=453, p<e-15) supports the notion that myelination is linked to the observed macrostructural volume changes, as predicted by an assumption that increased myelination leads to a white matter volume expansion[23]. The relatively modest, but consistent, effect size is partially explained on the basis that we only investigate the purely developmental associations and controlled for potentially confounding effects. However, our findings leave open a possibility that there might be additional microstructural factors driving the change in white matter macrostructure.

Voxel-wise analysis in gray matter revealed a more complex association between macrostructural development and myelination (Fig. 2b-c). We observed that the association is dependent on where a voxel is located in the tissue. An overall profile of consistently negative correlations (albeit relatively small) in gray matter zones close to the white matter boundary (0-2mm from GM/WM border: t=300, p<e-15) suggest that developmental

myelination may lead to a 'whitening' of gray matter, which in turn is likely to drive partial volume effects evident in a shrinkage of gray matter volume[23,24]. This means that a gray matter volume decline in deep layers during adolescence may well be driven by an increase in myelination within these same areas. This negative association was reduced with increased distance from the white matter boundary (Pearson r=0.3, p<e-15, Fig. 2c, bottom right panel). This suggests that ongoing myelination in superficial layers (i.e. close to the outer surface of the brain) contributes to an attenuated volume reduction and implies that developmental macrostructural change is the result of complex microstructural processes.

Compulsivity linked to reduced development in cingulate, dorsolateral and striatal MT

We next asked whether individual differences in the expression of symptoms, indicative of obsessive-compulsive traits, were associated with distinct developmental trajectories in myelin-sensitive MT growth. We employed a dimensional approach exploiting a heterogeneity within this otherwise healthy community sample. We computed a compound-score (first principal component, Supplementary Fig. 1a-f) from the two established obsessive-compulsive symptom questionnaires[25,26] available in our sample in order to aggregate a common score to index meaningful variation (cf. Supplementary Fig. 1). Top loading items on this score (subsequently called 'compulsivity') reflect compulsive behaviours, such as checking, and it was strongly aligned with total scores on our obsessive-compulsive questionnaires (Pearson correlations r>.8).

Assessing how compulsivity related to individual myelination over time, we found our compulsive measure was linked to altered MT growth primarily in frontal areas, with significant clusters in dorsolateral (superior frontal gyrus, GM: z=4.87, p=.009 FDR, [-23 34

49], WM: z=4.28, p<.05 FDR, [-24 -4 64]) and dorsomedial (anterior mid-cingulate, GM: z=4.1, p=.009 FDR, [18 1 58], WM: z=3.74, p<.05 FDR, [-25 1 37]) frontal cortices (Fig. 3a, Supplementary Table 3), both in cortical gray and adjacent superficial white matter. Importantly, more compulsive subjects showed reduced MT growth compared to less compulsive subjects. A similar pattern was seen in the left ventral striatum (z=3.9, p=.018 FDR, [-22 14 -9]) and adjacent white matter (z=4.2, p=.027 FDR, [21 -9 25], Fig. 3b). Intriguingly, the locations of reduced MT development were spatially centred in cingulate and ventral striatum, and this regional focus aligns with a specific fronto-striatal loop described in primate anatomical tracing[27] studies. This alignment with a well described anatomical circuit suggests compulsivity may relate to attenuated myelin-related developmental growth in this cingulate-striatal loop[13].

Reduced inferior prefrontal maturation trajectories in impulsivity

We next examined whether a common heterogeneity in impulsivity (as assessed using the well-established Barratt impulsiveness questionnaire total score; cf Supplementary Fig. 1f) is linked to individual growth of the myelin marker. In examining this linkage we opted to use a questionnaire measure over task-based measures of impulsivity because the former have been found to be more reliable (cf [28–32] for detailed discussion; stability subsample in this study[33] [N=63], BIS total: re-test reliability Pearson r=.76 for 1 year follow-up, reflection impulsivity decision parameter[34]: r=.16 for 6 months follow-up), reflecting a stable trait more likely to be linked to structural development. We found impulsivity was associated with reduction in adolescent MT growth with a strong focus on frontal areas, encompassing lateral (including inferior frontal gyrus, IFG; GM: z=1.65, p=.031 FDR, [-48 13 -4], WM: z=4.38, p=.015 FDR, [-27 39 -2]) and medial prefrontal areas (Fig. 4a, Supplementary Table 4; GM:

z=4.13, p=.031, [15 58 18], WM: z=3.69, p=.015, [-12 47 20]), both within gray and adjacent white matter (subcortical effects in Supplementary Fig. 5a).

The above finding suggests that while impulsivity and compulsivity are both linked to reduced myelin-related growth in prefrontal areas, these alterations have their peak expression in distinct anatomical regions (cingulate and dorsolateral vs inferior later and medial prefrontal cortex, for direct comparison cf. Supplementary Fig. 6). Interestingly, both compulsivity and impulsivity showed a reduced growth in the anterior insula (Supplementary Fig. 6), possibly expressing a common, transdiagnostic vulnerability.

We next investigated development-independent levels of myelination in impulsivity, indicating myelin-related differences that emerged before the commencement of our study. This is important because a pre-existing 'hyper-myelination' with the reduced ongoing growth would suggest a normalisation during adolescence, whereas a 'hypo-myelination' prior to adolescence onset would imply that a deficient myelination was further accentuated during adolescence. We found a main effect of impulsivity evident in hypo-myelination across several, primarily anterior prefrontal, brain areas including IFG (Fig. 4c, Supplementary Figure 5b, Supplementary Table 5). An overlap between these baseline effects and areas showing a reduced ongoing growth suggests that for impulsivity a gap in myelination may exist prior to adolescence, with this gap is widening further during a transition into adulthood. The same effects were found when analysing across the entire prefrontal cortex, where a reduced MT growth was linked to both compulsivity ($t(421)=1.99$, $p=.047$) and impulsivity ($t(421)=-2.80$, $p=.005$), but where a developmental, baseline hypo-myelination in impulsivity ($t(474)=2.30$, $p=.022$) is further accentuated during late adolescent development (no such effect was found for compulsivity: $t(427)=1.03$, $p=.30$, Supplementary Figure 7a-b).

Lastly, we examined how MT change related to the development of impulsivity traits. Although we did not see age-related change in impulsivity across the entire group, there was substantial variability within individuals (cf. Supplementary Fig. 1). We thus investigated whether myelin growth in IFG, a key region previously implicated in impulsivity[15], related to ongoing changes in impulsivity. We found that a change in IFG MT was negatively associated with impulsivity change (Pearson $r=-.27$, $p<.0003$, Fig. 4d), indicating that individuals with the least ongoing myelin growth had a worsening impulsivity over the course of the study (irrespective of other covariates, such as baseline impulsivity or age). Similar effects were also seen in prefrontal cortex when using a voxel-wise analysis (cf. Supplementary Figure 7c).

Discussion

Myelin enables fast and reliable communication within, and between, neuronal populations[35,36]. Using a longitudinal, repeated-measures, MRI scanning design in a developmental sample, we provide *in-vivo* evidence that myelination extends into adulthood as evident in a pronounced myelin-related whole-brain MT growth. We find that the macrostructural growth pattern closely resembles that expressed in our myelin marker. The positive association between these measures in white matter suggests that macrostructural volume change is, at least in part, driven by myelination. In gray matter, depth-dependent associations suggest that macrostructural volume reduction in adolescence is the result of multiple microstructural processes. In superficial layers, ongoing myelination seems to attenuate the impact of a pruning effect, leading to an apparent slowing in gray matter volume decline. In deeper layers, close to the gray-white matter boundary, ongoing myelination appears to contribute to an inflated estimate of volume reduction, with a myelin-induced 'whitening' of gray matter resulting in a misclassification of gray matter voxels (i.e. partial volume effects[23]), leading to an apparent volume reduction. This observation extends on recent cross-sectional studies that report age-related myelin increases in deep layers[7,24] and implies that developmental neuroimaging that avail of markers sensitive to specific microstructural processes[17] can provide more precise accounts of the likely mechanisms underlying adolescent and early adult brain development.

Critically, we found that individual differences in myelin-related MT growth during development is linked to common heterogeneity in compulsivity and impulsivity within an otherwise healthy sample. Both compulsivity and impulsivity were associated with a reduction in MT growth, and this reduction was almost exclusively present in fronto-striatal areas. In compulsivity, MT growth reduction was primarily expressed in dorsomedial and dorsolateral frontal regions as well as ventral striatum, whereas impulsivity was more tightly

linked to reduction in lateral and medial prefrontal growth. It is worth noting that variability in compulsivity/impulsivity does not reflect clinical impairment in this healthy sample[37]. Our findings extend on previous animal and patient studies that implicate lateral and medial prefrontal regions in attention-related functions[38] and ADHD[15,39]. It is also noteworthy that the regions implicated in compulsivity are reported to show altered function in OCD[40,41] and constitute prime targets for invasive OCD treatment interventions[42,43]. Critically, our findings of a reduced myelin growth linked to compulsivity suggest that differences in brain structural variables may not prevail during childhood (or only to a minor extent), but emerge during adolescence as a result of aberrant developmental processes.

Embracing a longitudinal developmental approach, as in this study, poses distinct developmental questions. In relation to impulsivity and compulsivity, we can ask how a stable trait is related to longitudinal change as well as baseline myelination differences, where the latter is more indicative of influences emerging prior to recruitment into our study. In the case of impulsivity, we found that ongoing growth occurred in similar regions that also express a difference in baseline myelination, advocating the presence of a pre-existing myelination gap in impulsivity that further expands during adolescence. This suggests that the mechanisms underlying impulsivity have long-lasting effects on brain development, possibly affecting myelination trajectories before adolescence onset with lasting effects into adulthood.

An extension of the approach outlined above poses the question as to how ongoing change in compulsivity and impulsivity relate to ongoing brain maturation (i.e. correlated change). Strikingly, we found that IFG growth change was indicative of change in impulsivity. Subjects who showed worsening of their impulsivity were also those who showed the least maturational myelin-related growth in IFG. Thus, during the transition into early adulthood even though impulsivity traits as a whole do not change at a population level,

individual psychiatric risk trajectories show meaningful variation, and this in turn is reflected in specific patterns of brain maturation.

In our study, we adopted a broad definition of impulsivity and compulsivity traits yet found links to myelin growth. This suggests reduced myelin-related growth in these areas may represent a developmental feature shared across multiple cognitive and/or genetic endophenotypes. This also implies that a more refined cognitive endophenotyping might yield spatially more defined developmental effects[44–46]. Compulsivity and impulsivity showed little overlap in our sample and this relative independence was also reflected in their impact on distinct fronto-striatal brain regions (with the exception of insula which showed a common growth reduction). These data leave open the possibility of a genetic pleiotropy, meaning that a shared genetic factor may drive both myelination and impulsivity/compulsivity, without a direct causal influence between brain and trait expression[47]. However, our correlated change finding that ongoing myelination in the IFG is directly related to how impulsivity evolves over time advocates for the possibility of a direct relationship between myelin-related maturation and impulsivity.

Variability in trait dimensions, such as compulsivity and impulsivity are often related to other variables known to affect brain structure. We examined how potential confounding factors, such as subject movement during scanning (Supplementary Figure 8a-f), alcohol consumption[45,46], recreational drug use, socio-economic status, intelligence (between subject differences and within-subject changes, Supplementary Fig. 9a-c) or ethnicity affected the link between compulsivity/impulsivity and MT growth. Importantly, none of these factors accounted for the observed effects (Supplementary Figure 9d).

A challenge for human neuroscience is to determine the cellular mechanisms that underlie macrostructural change *in-vivo*[48]. This has particular importance for developmental neuroscience where longitudinal, repeated-measures, approaches are critical for

understanding brain development[22]. Our focus in this study on a magnetization transfer (MT) saturation protocol as a proxy for myelin content is rooted in evidence of its sensitivity to myelin and related macromolecules[17], as well as the fact this measure is more robust to instrumental biases[20]. There is also evidence for a strong relationship between MT and myelin as measured in histological studies[18,19] and we have shown previously that MT is linked to myelin gene expression[7]. Our longitudinal findings extend the importance of MT as a myelin marker with relevance for individual differences. We show myelin-related effects are expressed in both cortical gray and adjacent white matter, but more pronounced in the former as found also in ex-vivo studies[4]. Taken together our findings suggest that MT is an important, albeit imperfect, indicator of myelin.

The transition into adulthood is a particularly vulnerable stage for the emergence of psychiatric illness[10]. Our findings suggest variability in the expression of compulsivity and impulsivity is tied to ongoing microstructural brain development. The brain's potential to dynamically adjust its myelination[49], for example as a function of training[50], points to the potential of interventions that target specific deviant trajectories. Such interventions might offer a novel therapeutic domain to lessen a developmental vulnerability to psychiatric disorder.

Acknowledgments:

A Wellcome Trust Cambridge-UCL Mental Health and Neurosciences Network grant (095844/Z/11/Z) supported this work. RJD holds a Wellcome Trust Investigator Award (098362/Z/12/Z). The UCL-Max Planck Centre is a joint initiative supported by UCL and the Max Planck Society (MPS). TUH is supported by a Wellcome Sir Henry Dale Fellowship (211155/Z/18/Z), a grant from the Jacobs Foundation, the Medical Research Foundation, and a 2018 NARSAD Young Investigator grant (27023) from the Brain & Behavior Research Foundation. MM receives support from the UCLH NIHR BRC. PF is in receipt of a National Institute for Health Research (NIHR) Senior Investigator Award (NF-SI-0514-10157), and was in part supported by the NIHR Collaboration for Leadership in Applied Health Research and Care (CLAHRC) North Thames at Barts Health NHS Trust. EB is in receipt of a National Institute for Health Research (NIHR) Senior Investigator Award, and was in part supported by the NIHR Cambridge Biomedical Research Centre (BRC). The Wellcome Centre for Human Neuroimaging is supported by core funding from the Wellcome Trust (203147/Z/16/Z). First, we thank R. Davis and FIL IT support for making large sample analysis feasible and more efficient. Thanks also to G. Prabhu. We thank specific experts for input in relation to applied and technical methods, particularly R. Dahnke, W. Penny and G. Ridgway, M. Callaghan, N. Weiskopf and B. Draganski, J. Ashburner and C. Gaser, G. Flandin, T. Nichols, B. Guillaume, J. Bernal-Rusiel, M. Völkle, C. Driver, A. Brandmeier, F. Dick, M. Betts, GJ. Will, and R. Kievit. Finally, GZ thanks E. Düzel for support at the DZNE. The views expressed are those of the authors and not necessarily those of the NHS, the NIHR or the Department of Health and Social Care

Author contributions

E.T.B., I.M.G., P.F., P.B.J., NSPN Consortium, M.M, and R.J.D. designed the experiment. G.Z., T.U.H. and NSPN Consortium performed the experiment and analysed the data. G.Z., T.U.H., U.L. and R.J.D. wrote the paper.

Competing Interest

E.T.B. is employed half-time by the University of Cambridge and half-time by GlaxoSmithKline and holds stock in GlaxoSmithKline. All other authors declare no competing financial interests.

References

1. Gogtay, N. *et al.* Dynamic mapping of human cortical development during childhood through early adulthood. *Proc. Natl. Acad. Sci. U. S. A.* **101**, 8174–8179 (2004).
2. Sowell, E. R., Thompson, P. M., Holmes, C. J., Jernigan, T. L. & Toga, A. W. In vivo evidence for post-adolescent brain maturation in frontal and striatal regions. *Nat. Neurosci.* **2**, 859–861 (1999).
3. Paus, T. Growth of white matter in the adolescent brain: myelin or axon? *Brain Cogn.* **72**, 26–35 (2010).
4. Miller, D. J. *et al.* Prolonged myelination in human neocortical evolution. *Proc. Natl. Acad. Sci. U. S. A.* **109**, 16480–16485 (2012).
5. Perrin, J. S. *et al.* Growth of white matter in the adolescent brain: role of testosterone and androgen receptor. *J. Neurosci. Off. J. Soc. Neurosci.* **28**, 9519–9524 (2008).
6. Petanjek, Z. *et al.* Extraordinary neoteny of synaptic spines in the human prefrontal cortex. *Proc. Natl. Acad. Sci. U. S. A.* **108**, 13281–13286 (2011).
7. Whitaker, K. J. *et al.* Adolescence is associated with genomically patterned consolidation of the hubs of the human brain connectome. *Proc. Natl. Acad. Sci.* **113**, 9105–9110 (2016).
8. Foulkes, L. & Blakemore, S.-J. Studying individual differences in human adolescent brain development. *Nat. Neurosci.* (2018). doi:10.1038/s41593-018-0078-4
9. Kessler, R. C. *et al.* Lifetime prevalence and age-of-onset distributions of mental disorders in the World Health Organization's World Mental Health Survey Initiative. *World Psychiatry Off. J. World Psychiatr. Assoc. WPA* **6**, 168–176 (2007).
10. Paus, T., Keshavan, M. & Giedd, J. N. Why do many psychiatric disorders emerge during adolescence? *Nat. Rev. Neurosci.* **9**, 947–957 (2008).

11. McCarthy, H. *et al.* Attention network hypoconnectivity with default and affective network hyperconnectivity in adults diagnosed with attention-deficit/hyperactivity disorder in childhood. *JAMA Psychiatry* **70**, 1329–1337 (2013).
12. Douaud, G. *et al.* A common brain network links development, aging, and vulnerability to disease. *Proc. Natl. Acad. Sci.* **111**, 17648–17653 (2014).
13. Robbins, T. W., Gillan, C. M., Smith, D. G., de Wit, S. & Ersche, K. D. Neurocognitive endophenotypes of impulsivity and compulsivity: towards dimensional psychiatry. *Trends Cogn. Sci.* **16**, 81–91 (2012).
14. de Wit, S. J. *et al.* Multicenter voxel-based morphometry mega-analysis of structural brain scans in obsessive-compulsive disorder. *Am. J. Psychiatry* **171**, 340–349 (2014).
15. Norman, L. J. *et al.* Structural and functional brain abnormalities in attention-deficit/hyperactivity disorder and obsessive-compulsive disorder: A comparative meta-analysis. *JAMA Psychiatry* **73**, 815–825 (2016).
16. Carlisi, C. O. *et al.* Comparative multimodal meta-analysis of structural and functional brain abnormalities in autism spectrum disorder and obsessive-compulsive disorder. *Biol. Psychiatry* (2016). doi:10.1016/j.biopsych.2016.10.006
17. Weiskopf, N., Mohammadi, S., Lutti, A. & Callaghan, M. F. Advances in MRI-based computational neuroanatomy: from morphometry to in-vivo histology. *Curr. Opin. Neurol.* **28**, 313–322 (2015).
18. Schmierer, K., Scaravilli, F., Altmann, D. R., Barker, G. J. & Miller, D. H. Magnetization transfer ratio and myelin in postmortem multiple sclerosis brain. *Ann. Neurol.* **56**, 407–415 (2004).
19. Turati, L. *et al.* In vivo quantitative magnetization transfer imaging correlates with histology during de- and remyelination in cuprizone-treated mice. *NMR Biomed.* **28**, 327–337 (2015).

20. Callaghan, M. F., Helms, G., Lutti, A., Mohammadi, S. & Weiskopf, N. A general linear relaxometry model of R1 using imaging data. *Magn. Reson. Med.* **73**, 1309–1314 (2015).
21. Campbell, J. S. W. *et al.* Promise and pitfalls of g-ratio estimation with MRI. *NeuroImage* (2017). doi:10.1016/j.neuroimage.2017.08.038
22. Raz, N. & Lindenberger, U. Only time will tell: cross-sectional studies offer no solution to the age-brain-cognition triangle: comment on Salthouse (2011). *Psychol. Bull.* **137**, 790–795 (2011).
23. Paus, T. Mapping brain maturation and cognitive development during adolescence. *Trends Cogn. Sci.* **9**, 60–68 (2005).
24. Natu, V. S. *et al.* Apparent thinning of visual cortex during childhood is associated with myelination, not pruning. *bioRxiv* 368274 (2018). doi:10.1101/368274
25. Burns, G. L., Keortge, S. G., Formea, G. M. & Sternberger, L. G. Revision of the Padua Inventory of obsessive compulsive disorder symptoms: Distinctions between worry, obsessions, and compulsions. *Behav. Res. Ther.* **34**, 163–173 (1996).
26. Foa, E. B. *et al.* The Obsessive-Compulsive Inventory: Development and validation of a short version. *Psychol. Assess.* **14**, 485–496 (2002).
27. Haber, S. N. Corticostriatal circuitry. *Dialogues Clin. Neurosci.* **18**, 7–21 (2016).
28. Palminteri, S. & Chevallier, C. Can We Infer Inter-Individual Differences in Risk-Taking From Behavioral Tasks? *Front. Psychol.* **9**, (2018).
29. Pedroni, A. *et al.* The risk elicitation puzzle. *Nat. Hum. Behav.* **1**, 803 (2017).
30. Frey, R., Pedroni, A., Mata, R., Rieskamp, J. & Hertwig, R. Risk preference shares the psychometric structure of major psychological traits. *Sci. Adv.* **3**, e1701381 (2017).
31. Moutoussis, M. *et al.* Change, stability, and instability in the Pavlovian guidance of behaviour from adolescence to young adulthood. *PLOS Comput. Biol.* **14**, e1006679 (2018).

32. Shahar, N. *et al.* Improving the reliability of model-based decision-making estimates in the two-stage decision task with reaction-times and drift-diffusion modeling. *PLOS Comput. Biol.* (in revision).
33. Kiddle, B. *et al.* Cohort profile: The NSPN 2400 Cohort: a developmental sample supporting the Wellcome Trust NeuroScience in Psychiatry Network. *Int. J. Epidemiol.* (2017). doi:10.1093/ije/dyx117
34. Moutoussis, M., Bentall, R. P., El-Deredy, W. & Dayan, P. Bayesian modelling of Jumping-to-Conclusions bias in delusional patients. *Cognit. Neuropsychiatry* **16**, 422–447 (2011).
35. Virchow, R. Ueber das ausgebreitete Vorkommen einer dem Nervenmark analogen Substanz in den thierischen Geweben. *Arch. Für Pathol. Anat. Physiol. Für Klin. Med.* **6**, 562–572 (1854).
36. Bunge, R. P. Glial cells and the central myelin sheath. *Physiol. Rev.* **48**, 197–251 (1968).
37. Holmes, A. J. & Patrick, L. M. The Myth of Optimality in Clinical Neuroscience. *Trends Cogn. Sci.* **22**, 241–257 (2018).
38. Rubia, K. 'Cool' inferior frontostriatal dysfunction in attention-deficit/hyperactivity disorder versus 'hot' ventromedial orbitofrontal-limbic dysfunction in conduct disorder: a review. *Biol. Psychiatry* **69**, e69-87 (2011).
39. Hauser, T. U. *et al.* Role of the Medial Prefrontal Cortex in Impaired Decision Making in Juvenile Attention-Deficit/Hyperactivity Disorder. *JAMA Psychiatry* (2014).
40. Hauser, T. U. *et al.* Increased fronto-striatal reward prediction errors moderate decision making in obsessive–compulsive disorder. *Psychol. Med.* 1–13 (2017). doi:10.1017/S0033291716003305
41. Gillan, C. M. *et al.* Functional neuroimaging of avoidance habits in obsessive-compulsive disorder. *Am. J. Psychiatry* **172**, 284–293 (2015).

42. Dougherty, D. D. *et al.* Prospective long-term follow-up of 44 patients who received cingulotomy for treatment-refractory obsessive-compulsive disorder. *Am. J. Psychiatry* **159**, 269–275 (2002).
43. Figee, M. *et al.* Deep brain stimulation restores frontostriatal network activity in obsessive-compulsive disorder. *Nat. Neurosci.* **16**, 386–387 (2013).
44. Boedhoe, P. S. W. *et al.* Distinct Subcortical Volume Alterations in Pediatric and Adult OCD: A Worldwide Meta- and Mega-Analysis. *Am. J. Psychiatry* appiajp201616020201 (2016). doi:10.1176/appi.ajp.2016.16020201
45. Whelan, R. *et al.* Adolescent impulsivity phenotypes characterized by distinct brain networks. *Nat. Neurosci.* **15**, 920–925 (2012).
46. Holmes, A. J., Hollinshead, M. O., Roffman, J. L., Smoller, J. W. & Buckner, R. L. Individual Differences in Cognitive Control Circuit Anatomy Link Sensation Seeking, Impulsivity, and Substance Use. *J. Neurosci. Off. J. Soc. Neurosci.* **36**, 4038–4049 (2016).
47. Pingault, J.-B. *et al.* Using genetic data to strengthen causal inference in observational research. *Nat. Rev. Genet.* **19**, 566–580 (2018).
48. Lerch, J. P. *et al.* Studying neuroanatomy using MRI. *Nat. Neurosci.* **20**, 314–326 (2017).
49. Franklin, R. J. M. & ffrench-Constant, C. Remyelination in the CNS: from biology to therapy. *Nat. Rev. Neurosci.* **9**, 839–855 (2008).
50. Sampaio-Baptista, C. *et al.* Motor skill learning induces changes in white matter microstructure and myelination. *J. Neurosci. Off. J. Soc. Neurosci.* **33**, 19499–19503 (2013).

.

494

495

496

497

Figure 1. Developmental growth of myelin-sensitive MT into early adulthood. Transitioning into adulthood is characterised by marked increases in a myelin marker within cortical gray **(a)**, white **(b)** and subcortical gray matter **(c)**. Statistical maps of voxel-wise MT saturation show growth with time/visit (longitudinal) or age (cross-sectional; for specific effects of covariates, e.g. time/visit, age, sex, interactions etc., see supplementary information). **(a)** Gray matter MT growth (top row; statistical z-maps, $p<.05$ FDR corrected, sampling-based correction reported in Supplementary Table 1, cf Supplementary Fig. 2c, n=497/288 scans/subjects for a-c, 51.7% female) is strongest in parietal, lateral temporal, posterior and middle cingulate, but is also present in prefrontal cortex. Longitudinal model in angular gyrus peak (mean across a 6mm sphere; coloured lines in left data plot; x-axis: relative time of scan) and adjusted data (uncoloured) shows an MT growth in both sexes, with a marked sex difference reflecting greater MT in females (see Supplementary Fig. 3c for region-specific sex differences). Corresponding cross-sectional model predictions in the same region show a similar increase with age (right data plot; y-axis: MT; x-axis: mean age over visits). **(b)** MT growth in adjacent cortical white matter is most pronounced in cingulate and parieto-temporal cortex with a coarse topographical correspondence to the gray matter MT effects. **(c)** Subcortical gray matter nuclei express MT age effects in striatum, pallidum, thalamus, amygdala and hippocampus (cf Fig. 2a-b). This growth is most pronounced in amygdala, ventral (max z-value voxel [z=4.81, p=.004 FDR], [MNI: 20 13 -11]) and posterior (z=4.47, p=0.004 FDR, [MNI: -31 -19 3]) striatum suggesting ongoing myelin-associated changes in both cortical and subcortical brain structures.

Figure 2. The relation between macrostructural and microstructural brain development. **(a)** Coronal sections through prefrontal (left panels), striatal (middle) and thalamus/hippocampus (right; MNI: y=15, 12, -14) show more myelin-related MT in white

than in gray matter with a clearly preserved white-gray matter boundary (top row, n=497/288 scans/subjects in a-c, 51.7% female). Developmental change in MT (second row) shows an increase in myelin marker in both tissues, with a stronger growth in gray matter areas. Developmental change in macrostructural brain volume (third row) shows a characteristic cortical shrinkage (blue colours) in gray, but an expansion in core and frontal white matter (red colours; cf Supplementary Fig. 4). Only hippocampal gray matter shows an opposite effect with continuing gray matter growth up to the verge of adulthood. **(b)** Association between microstructural myelin growth and macrostructural volume change. A positive association throughout whole-brain white matter supports the notion that myelination contributes to white matter expansion. In gray matter, a predominantly negative association in deep layers points to partial volume effects at the tissue boundary and positive associations in superficial layers (correlation was obtained from posterior covariance of beta parameters in sandwich estimator model simultaneously including longitudinal observations of both imaging modalities). **(c)** Association as a function of Euclidean distance to GM/WM boundary. Microstructural growth (top row, Pearson's correlation and p-values from corresponding t-distribution based on n=336164/118502 voxels in cortical gray/white matter) shows consistent myelin-related growth in both tissues, but opposite macrostructural volume change (middle row). Association between micro- and macrostructural growth is positive in white matter, independent of distance. In gray matter, the mean association changes from negative in deep layers (i.e. myelin MT change associated with reduced gray matter volume) to more positive associations in superficial layers (i.e. MT associated with a tendency to more gray matter volume).

Figure 3. Compulsivity is related to altered fronto-striatal MT growth. Longitudinal developmental change of our myelin marker is reduced in high compulsive subjects. **(a)**

Aggregate compulsivity score is related to decreased MT growth in dorsolateral frontal gray matter (upper panel; p<.05, FDR and bootstrapping corrected; Supplementary Table 3, n=452/246 scans/subjects in a-b with available compulsivity, 50.4% female) and adjacent white matter, as well as cingulate cortex (lower panel; blue colours depicting negative time by compulsivity interactions). Subjects with higher compulsivity scores (light yellow) compared to low scoring subjects (dark red) express significantly less MT growth over visits (coloured lines in right panel indicate the interaction effect; y-axis: MT; x-axis: time of scan in years relative to each subject's mean age over visits). **(b)** The above slowing in cortical myelin-related growth is mirrored by a decreased developmental growth in subcortical ventral striatum (left panel) and the adjacent white matter (right panel). These findings indicate young people with high compulsive traits express slower maturational myelin-related change in a fronto-striatal network comprising cingulate cortex and ventral striatum.

Figure 4. Decreased frontal growth in myelin-sensitive MT in impulsivity. Myelin marker (MT) in frontal lobe is linked to impulsivity traits. **(a)** Impulsivity is associated with reduced growth of MT in lateral (inferior and middle frontal gyrus), medial prefrontal areas, motor/premotor and parietal areas in both gray (top panel) and adjacent white matter (bottom panel) depicting negative time by impulsivity interactions (z maps, p<.05 FDR and bootstrapping corrected, Supplementary Table 4, n=497/288 subjects/scans in a-c, 51.7% female). **(b)** Plot shows subjects with higher impulsivity (light yellow) compared to low scoring subjects (dark red) express significantly less MT growth over visits (coloured lines in right panel indicate the interaction effect; y-axis: MT; x-axis: time of scan in years relative to each subject's mean age over visits). **(c)** More impulsive subjects show a local decrement in baseline myelin marker (peak middle frontal gyrus, p<0.05, FDR and bootstrapping corrected, Supplementary Table 5) in lateral and orbitofrontal areas (fixed for other

covariates, e.g. time/visits, mean age of subject, sex). Right panel shows the plot of MT in this peak voxel over impulsivity (x-axis, z-scored) and with adjusted data (gray/black) and model predictions (red/orange, effects of interest: intercept, impulsivity, sex by impulsivity). **(d)** Bilateral IFG not only shows a reduced myelination process for higher impulsivity (as shown in a, b), but this reduced growth rate is more strongly expressed in subjects who manifest an accentuated impulsivity growth over study visits, such that subjects who manifest an even more restricted growth in myelin become more impulsive (Pearson's correlation and p-value from corresponding t-distribution based on n=188 independent subjects with available follow-up scans).

Online Methods

Study design & participants

The NSPN study[33] used an accelerated longitudinal design to investigate variability in compulsivity and impulsivity traits and brain maturation during adolescence and early adulthood. Participants were recruited in London and Cambridgeshire from schools, colleges, primary care services and through advertisement. Subjects were sampled in six age bins 14-15y, 16-17y, 18-19y, 20-21y, and 22-24y, with roughly balanced numbers (overall age mean (std) 19.45 (2.85) years). Each age bin was balanced for sex and ethnicity (relative to the local population). From the 2406 participants that took part in the study and which filled out socio-demographic information and questionnaires at least once, 318 healthy subjects (~60 subjects per age bin) participated in the MRI arm. Subjects with self-reported pervasive neurological, developmental or psychiatric disorders were excluded from the recruitment. After rigorous visual quality control and excluding 10% of scans with highest during-scan motion (cf. Supplementary Fig. S8 for details) of all 558 processed imaging datasets, 61 scans from 30 subjects had to be discarded due to severe artefacts. We finally analysed 497 available brain scans from 288 (149 female) healthy individuals that passed rigorous quality control. In particular, data from 100, 167, and 21 subjects with one, two or three visits per person were available, with mean (standard deviation) follow-up interval of 1.3 (0.32) years between first and last visit. The study was approved by the Cambridge Central Research Ethics Committee (12/EE/0250) and all participants (if <16y also their legal guardian) gave written informed consent.

Assessing compulsivity and impulsivity

To examine the effects of compulsivity and impulsivity traits on myelin development, we analysed psychometric questionnaires that were handed out to the participants over the

course of the study. A detailed description of the assessment waves and the overall structure of the NSPN study is provided elsewhere[33]. As an index of impulsivity, we used the Barratt Impulsiveness Scale (BIS)[51] total score, a well-established and calibrated measure of general impulsivity. To assess compulsivity, we built a composite score (using principal component analysis (PCA), cf supplementary information) from two established obsessive-compulsive questionnaires that were available in this study (Supplementary Fig. 1a-e, revised Obsessive-Compulsive Inventory, OCI-R[26], and revised Padua Inventory, PI-WSUR[25]).

Questionnaires were assessed at several times throughout the study. BIS was completed at home by participants on up to three occasions (ca 1 year between assessments), with the first assessment wave taking place before initial scanning. PI-WSUR was also completed at home during waves 2 and 3. OCI-R was assessed on the day of the second MRI scan. Per construction, the considered psychometric questionnaires aim at measuring stable subject-specific traits but cognitive constructs could as well change over the course of this longitudinal study. In our sample, linear mixed-effects modelling (LME, cf supplementary information) revealed that both indices did not substantially change during the study period while accounting for covariates and confounds, which motivated our use of aggregated scores (LME intercepts) for most of the subsequent MRI analyses on impulsivity. Compulsivity and impulsivity trait measures showed a weak (Pearson) correlation r=0.119 in the large behavioural sample, supporting a notion of rather independent dimensions (less than 1.4% shared variance, cf Supplementary Fig. 1).

MRI data acquisition and longitudinal preprocessing

Brain scans were acquired using the multi-echo FLASH MPM protocol[52] on three 3T Siemens Magnetom TIM Trio MRI systems located in Cambridge and London. Comparability between scanners was assessed prior to study onset (for more details, cf [33])

and differences between scanners were accounted for by adding scanner as covariates in our analyses. Isotropic 1mm MT maps were collected to quantify local changes in gray and adjacent white matter and all image processing was performed using SPM12 (Wellcome Centre for Human Neuroimaging, London, UK, http://www.fil.ion.ucl.ac.uk/spm), the h-MRI toolbox for SPM[53,54] (www.hmri.info), Computational Anatomy toolbox (CAT, http://www.neuro.uni-jena.de/cat/) and custom made tools (cf code availability statement).

Magnetization transfer saturation (MT) maps provide semi-quantitative maps for myelin and related macro-molecules, and correlate highly with myelin content in histological studies[18,19]. MT shows a high sensitivity to actual microstructural changes such as myelin and thus overcomes limitations in previous methods, such as diffusion tensor imaging, which measure microstructural change only indirectly through assessing diffusivity[55]. It was also found to be more robust than earlier protocols such as magnetization transfer ratio[20]. This is important also because myelin patterns are defining for brain anatomy and are used for subdividing brain structures[56,57].

Since longitudinal neuroimaging is prone to artefacts due to registration inconsistency, scanner inconsistencies and age-related deformations of the brains, we developed advanced processing pipelines in order to detect the changes of interest and achieve unbiased results. To assess the microstructural myelin-related MT changes during development, we used a longitudinal processing pipeline with the following steps (Supplementary Fig. 2a). To normalise images, we performed a symmetric diffeomorphic registration for longitudinal MRI[58]. The optimization is realized within one integrated generative model and provides consistent estimates of within-subject brain deformations over the study period and a midpoint image for each subject. The midpoint image is subsequently segmented into gray matter (GM), white matter (WM) and cerebrospinal fluid using CAT. MT maps from all time-points were then normalized to MNI space using geodesic

shooting[59,60], spatially smoothed preserving GM/WM tissue boundaries[54], and manually as well as statistically quality checked using a proxy for during-scan motion (cf. Supplementary Fig. 8) and covariance-based sample homogeneity measures (as implemented in CAT). Lastly, we constructed masks for both gray and adjacent white matter using anatomical atlases for subsequent analysis (cf. illustrated in Supplementary Fig. 2b).

To relate these quantitative (Voxel-Based Quantification, VBQ) to more conventional metrics (i.e. Voxel-Based Morphometry), we normalized tissue segment maps to account for existing differences and ongoing changes of local volumes using within- and between-subjects modulation. The obtained maps were spatially smoothed (6 mm FWHM). All analyses were conducted in voxel-space, and then projected onto surface space for illustration purposes. Voxel-wise result maps can be inspected online (cf data availability statement).

In this paper, we focused on the developmental VBQ analysis of myelin-sensitive MT. Since this is the first longitudinal study with this marker, effects of demographics (time/visits, age and sex) as well as impulsivity and compulsivity were considered on the whole-brain level. The analyses were particularly aimed at exploring MT in gray matter and the adjacent superficial white matter tissue. In order to define disjunct but adjacent gray and white matter regions for voxel-based analysis in the MNI template space, the gray and white matter tissue classes of the template were thresholded with 0.5, resulting in an approximately symmetric GM/WM boundary, i.e. with roughly 0.5 probability for each tissue class for voxels on the boundary (shown in Fig. 2). The resulting (non-overlapping) canonical gray and white matter tissue masks are not expected to be biased towards either gray or white matter and thus avoid over- or underestimation on both tissue classes. The subcortical gray and white matter masks were computed analogously.

Longitudinal design specification, MT image, and statistical analyses

In this study, we employed a longitudinal observational design to examine myelin-related MT development in late adolescence and early adulthood. Traditional cross-sectional approaches employ between-subject measures to study age-related differences rather than within-subject changes. These can be affected by biases[61], such as cohort differences[62,63] or selection bias[64], and typically require additional assumptions, such as (a) the age-related effect in the sample is an unbiased estimate of the group level average of individual within-subject effects of time or (b) all subjects change in the same way. Here, we follow recent analysis recommendations[65], taking the advantage of the accelerated longitudinal design in which we study separately (in one joint model) (a) how the individual brain changes over time/visits (from baseline to follow up(s)) and (b) how it varies with mean age of different subjects in the study, and their interaction. To do so, we used the accurate and efficient Sandwich Estimator (SwE)[65] method for voxel-based longitudinal image analysis (http://www.nisox.org/Software/SwE; cf supplementary information). Similar to common cross-sectional general linear modelling (GLM) approaches, this so-called marginal model describes expected variability as a function of predictors in a design matrix, while additionally accounting for correlations due to repeated measurements and unexplained variations across individuals as an enriched error term (illustrated in Supplementary Fig. 2b),

In our developmental analyses, we focused on the factors time/visits and mean age of the individual (over all visits). Moreover, in order to investigate if, and how, compulsivity and impulsivity traits are related to brain trajectories and altered growth we enriched the models by adding a main effect of trait (compulsivity/impulsivity), as well as their interaction with change over time/visits. The latter metric allowed us to assess how MT growth is associated with compulsivity and impulsivity traits (e.g., lower MT growth in high compulsives), whereas the former indicates how a trait relates to overall MT differences across individuals, independent of all other covariates (time, mean age of a subject over all

scans, sex, etc.). Unless specifically mentioned, all analyses were performed in a dimensional manner using the subjects' trait scores directly rather than comparing median-split groups. Notably, in addition to including effects time/visit, mean age of subject (further denoted age_mean), and compulsivity/impulsivity traits, all models were tested for indications of effects of (a) other relevant demographic factors, especially sex and socioeconomic status (as measured by national poverty index[66]); (b) effects of during scan motion as indicated by standard deviation of R2* exponential decay residuals in white matter areas (cf. supplementary methods and Supplementary Fig. 8a-c); (c) non-linearites (accelerations/deceleration) of brain changes (across the study age range) and age-related trajectories, especially using time by age_mean interactions, and quadratic/cubic effects of age_mean; and (d) all first order interactions among all previous covariates. All image analysis results were based on one-sided Wald-tests implementing the research questions (such as hypothesized developmental growth or trait-related impairment) described above. More detailed notes on longitudinal modelling and design specification can be found in supplementary information.

There were no indications of substantial nonlinearities for myelin-sensitive MT (cf Supplementary Fig. 3d), but for volumes (cf Supplementary Fig. 4b). Demographic covariates and confounds (motion, total intracranial volume, scanner, socioeconomic status) were included in all models, and additional interactions of covariates were included when showing significant effects. This is intended to account for potential confounding effects of residual head size variations induced by tissue-weighted smoothing of quantitative MT analysis during morphometric analysis. Additionally, this allows utilisation of a consistent design (and power) across modalities. We additionally examined the effects of potentially confounding covariates, such as alcohol consumption, recreational drug use, ethnicity ('white' vs 'other'), and IQ, but did not find any effect on our main results (cf.

735 Supplementary Fig. 9d). We controlled for the False Discovery Rate (FDR) during
736 corrections for multiple comparisons in all image analyses. We additionally report
737 bootstrapping-based results (cf. Supplementary Fig. 2c; Supplementary Tables 1 & 3-5). We
738 illustrate local trajectories using model predictions based on parameters and data averaged in
739 6mm spheres around peak effects. These model predictions are focussed on specific effects of
740 interest (e.g. study visit or impulsivity) while the data is shown adjusting for effects of no-
741 interest (e.g. other covariates and confounds, c.f. illustrated in Supplementary Fig. 4b).
742 To examine the topographical similarity of growth effects in gray and adjacent white
743 matter, we assessed the correlation between GM and nearest neighbouring WM voxels
744 (significance tested using 1000 permutation tests).
745 The sample size was conceived by NSPN consortium during the design of this study
746 based on the developmental studies that were available at the time[33]. We used normalisation
747 procedures (z-scoring and boxcox-transformation) for the psychometric data to align with the
748 normality assumptions of our tests. In addition, all qMRI image analysis were additionally
749 examined using sampling methods that do not assume normality of data distributions to allow
750 valid inference. Our study had an observational design and no randomization of subgroups
751 was used. Our study design also implied that data collection and analysis were not performed
752 blinded.
753
754 *Analysis of macrostructural changes and MT/Volume associations*
755 To relate the findings from our microstructural myelin marker (MT) to traditional
756 macrostructural markers (GM/WM volume), we performed analogue analyses (using VBM[67])
757 as described above on traditional normalized tissue segment maps. To quantify how
758 developmental changes of macro- to microstructural parameters correlate, we specified a
759 multi-modal SwE model including all volumetric and MT scans in a joint (block-diagonal)

760 design matrix with all covariates separately for each modality. Developmental effects within
761 each modality are defined by respective *time/visit* and *age_mean* beta estimates of those
762 regressors of the design matrix. After SwE model estimation, the posterior covariance of
763 these beta parameters from volume and MT modalities were calculated and transformed into
764 correlation (see Fig. 2b).
765
766 *Assessing wide-spread effects of compulsivity and impulsivity*
767 To assess the effects of development and compulsivity/impulsivity on myelin-
768 sensitive MT across the entire frontal lobe (GM, WM separately), we used linear mixed-
769 effects modelling (LME, cf supplementary information). Besides assessing the effects of
770 *time/visit* and *time* by (continuous) *trait* interactions, we calculated the model predictions
771 over the study period while accounting for covariates[68]. Random-effect intercepts were
772 included and proved optimally suited using likelihood ratio tests. Global frontal MT was
773 analysed separately for each dimension (shown in Supplementary Fig. 7a) and jointly with
774 both dimensions (and their interaction) included in the design (Supplementary Fig. 7b). For
775 both of these global models, we used discrete (median split bivariate traits: low vs. high) for
776 simplified illustration although continuous variables were used during modelling.
777
778 *Analysis of correlated changes of brain and impulsivity*
779 To assess whether MT development was related individual changes in impulsivity, we
780 conducted a hypothesis-driven analysis of the bilateral IGF (anatomically defined). This LME
781 analysis provides information about whether changes in impulsivity also reflect how quickly
782 a brain region myelinates during the study period. The LME model used IFG MT, rates of
783 change in IFG MT, time, their interaction, as well as the above introduced covariates as fixed
784 effect to predict the dependent variable impulsivity score. We visualize the observed

correlated changes using simple correlations. In addition, we conducted exploratory voxel-wise correlated change analyses. Time-varying BIS scores were decomposed in purely within- and between-subject components and entered as regressors in voxel-wise SwE modelling of myelin-sensitive MT (in addition to covariates *time/visits*, *age_mean*, *sex*, *interactions and confounds*, cf. supplemental information).

Analysis of MT peak effect specificity for both traits and compulsivity subtests

Above described voxel-based SwE analysis assessed whether there is region-specific growth in myelin-sensitive MT and compulsivity and impulsivity related impairment of the ongoing myelination process. However, here we complemented this by a subsequent analysis of MT in observed fronto-striatal peak effects (Fig. 3 and 4) and global frontal MT using LME modelling. More specifically, we were interested in specificity of local brain trajectories associated with each or eventually both impulsivity and compulsivity *traits*. The fixed effects design was specified with *X = [intercept, time/visit, time by trait interaction, trait, age_mean, sex, socioeconomic status, confounders]* (similar to the mass-univariate SwE models above). We explored the potential interaction of both dimensions, in addition to the separate modelling (presented in Fig. 3 & 4) a joint model was specified including both *traits* simultaneously, as well as their interaction (not found to be significant), and their respective interactions with *time/visits.* By inclusion of both effects of *trait* as well as their *time by trait interaction*, we accounted for potential baseline and rate-of-change differences related to both trait dimensions simultaneously rendering coefficients/statistics specific for each dimension. Random effects were restricted to intercepts. The specificity of MT (averaged in 6mm sphere around peaks observed in voxel-based SwE analysis above) for compulsivity and impulsivity is presented in Supplementary Fig. 6. Finally, we assessed the specificity of two available compulsivity scores, OCI-R and PI-WSUR for the observed reduced MT growth effects using

our compulsivity dimension (from PCA). Thus, we explored each subscore's main effect and time/visit interactions on local MT trajectories (in averaged in 6mm spheres of peaks presented in Fig. 3a) as detailed in Supplementary Fig. 5c.

Reporting Summary

Further information on research design is available in the Nature Research Reporting Summary linked to this article.

Data Availability Statement

Whole-brain results are available for inspection online on Neurovault (https://neurovault.org/collections/YAHZLJRW/). Data for this specific paper has been uploaded to the Cambridge Data Repository (https://doi.org/10.17863/CAM.12959) and password protected. Our participants did not give informed consent for their measures to be made publicly available, and it is possible that they could be identified from this data set. Access to the data supporting the analyses presented in this paper will be made available to researchers with a reasonable request to openNSPN@medschl.cam.ac.uk or the corresponding authors [G.Z., T.U.H.].

Code availability

Custom made SPM pipeline code for longitudinal VBM and VBQ processing is provided along with the manuscript (https://github.com/gabrielziegler/gz/tree/master/nspn_mpm_prepro_code_and_example). The code aims at transparency of applied procedures but is not intended for clinical use. It is free but copyright software, distributed under the terms of the GNU General Public Licence

as published by the Free Software Foundation (either version 2, or at your option, any later version). For any questions and requests please contact gabriel.ziegler@dzne.de

Methods-only references

51. Patton, J. H., Stanford, M. S. & Barratt, E. S. Factor structure of the Barratt impulsiveness scale. *J. Clin. Psychol.* **51**, 768–774 (1995).
52. Weiskopf, N. *et al.* Quantitative multi-parameter mapping of R1, PD*, MT, and R2* at 3T: a multi-center validation. *Front. Neurosci.* **7**, (2013).
53. Callaghan, M. F. *et al.* Widespread age-related differences in the human brain microstructure revealed by quantitative magnetic resonance imaging. *Neurobiol. Aging* **35**, 1862–1872 (2014).
54. Draganski, B. *et al.* Regional specificity of MRI contrast parameter changes in normal ageing revealed by voxel-based quantification (VBQ). *NeuroImage* **55**, 1423–1434 (2011).
55. Jones, D. K., Knösche, T. R. & Turner, R. White matter integrity, fiber count, and other fallacies: The do's and don'ts of diffusion MRI. *NeuroImage* **73**, 239–254 (2013).
56. Donahue, C. J., Glasser, M. F., Preuss, T. M., Rilling, J. K. & Van Essen, D. C. Quantitative assessment of prefrontal cortex in humans relative to nonhuman primates. *Proc. Natl. Acad. Sci. U. S. A.* **115**, E5183–E5192 (2018).
57. Glasser, M. F. *et al.* A multi-modal parcellation of human cerebral cortex. *Nature* **536**, 171–178 (2016).
58. Ashburner, J. & Ridgway, G. R. Symmetric diffeomorphic modeling of longitudinal structural MRI. *Front. Neurosci.* **6**, 197 (2012).
59. Ashburner, J. A fast diffeomorphic image registration algorithm. *NeuroImage* **38**, 95–113 (2007).
60. Ashburner, J. & Friston, K. J. Diffeomorphic registration using geodesic shooting and Gauss–Newton optimisation. *NeuroImage* **55**, 954–967 (2011).
61. Neuhaus, J. M. & Kalbfleisch, J. D. Between- and Within-Cluster Covariate Effects in the Analysis of Clustered Data. *Biometrics* **54**, 638–645 (1998).

62. Hoffman, L., Hofer, S. M. & Sliwinski, M. J. On the confounds among retest gains and age-cohort differences in the estimation of within-person change in longitudinal studies: a simulation study. *Psychol. Aging* **26**, 778–791 (2011).
63. Sliwinski, M., Hoffman, L. & Hofer, S. M. Evaluating Convergence of Within-Person Change and Between-Person Age Differences in Age-Heterogeneous Longitudinal Studies. *Res. Hum. Dev.* **7**, 45–60 (2010).
64. Lash, T. L., Fox, M. P. & Fink, A. K. *Applying Quantitative Bias Analysis to Epidemiologic Data*. (Springer, 2009).
65. Guillaume, B. *et al.* Fast and accurate modelling of longitudinal and repeated measures neuroimaging data. *NeuroImage* **94**, 287–302 (2014).
66. Personal and household finances - Office for National Statistics. Available at: https://www.ons.gov.uk/peoplepopulationandcommunity/personalandhouseholdfinances/. (Accessed: 17th October 2018)
67. Ashburner, J. & Friston, K. J. Voxel-based morphometry--the methods. *NeuroImage* **11**, 805–821 (2000).
68. Gelman, A. *et al. Bayesian Data Analysis, Third Edition*. (Chapman and Hall/CRC, 2013).

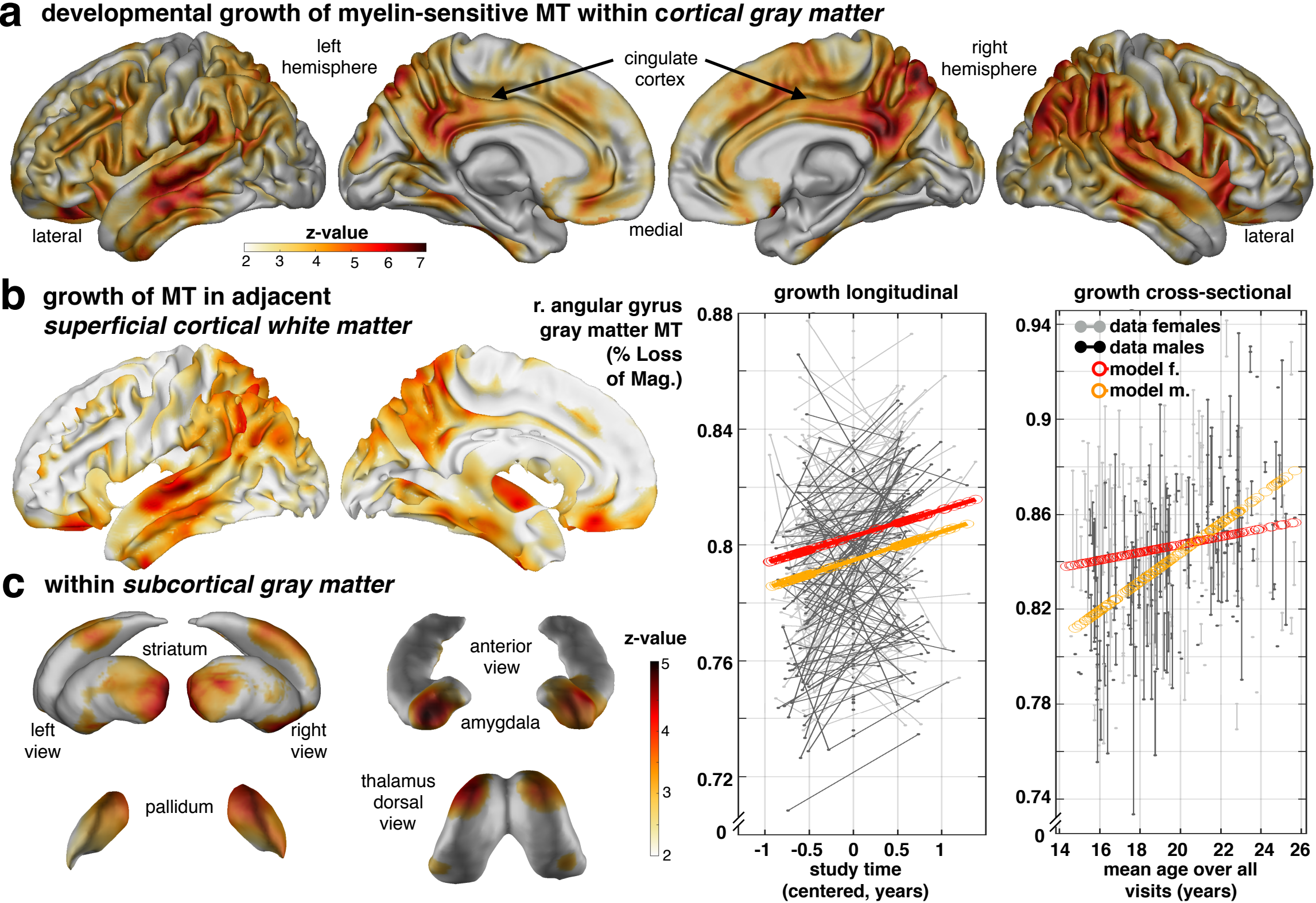
a
developmental growth of myelin-sensitive MT within cortical gray matter
left hemisphere
cingulate cortex
right hemisphere
lateral
medial
lateral
z-value
2 3 4 5 6 7
b
growth of MT in adjacent superficial cortical white matter
r. angular gyrus gray matter MT (% Loss of Mag.)
c
within subcortical gray matter
striatum
left view
right view
anterior view
amygdala
pallidum
thalamus dorsal view
z-value
5 4 3 2
growth longitudinal
0.88 0.84 0.8 0.76 0.72 0
-1 -0.5 0 0.5 1
study time (centered, years)
growth cross-sectional
data females
data males
model f.
model m.
0.94 0.9 0.86 0.82 0.78 0.74 0
14 16 18 20 22 24 26
mean age over all visits (years)

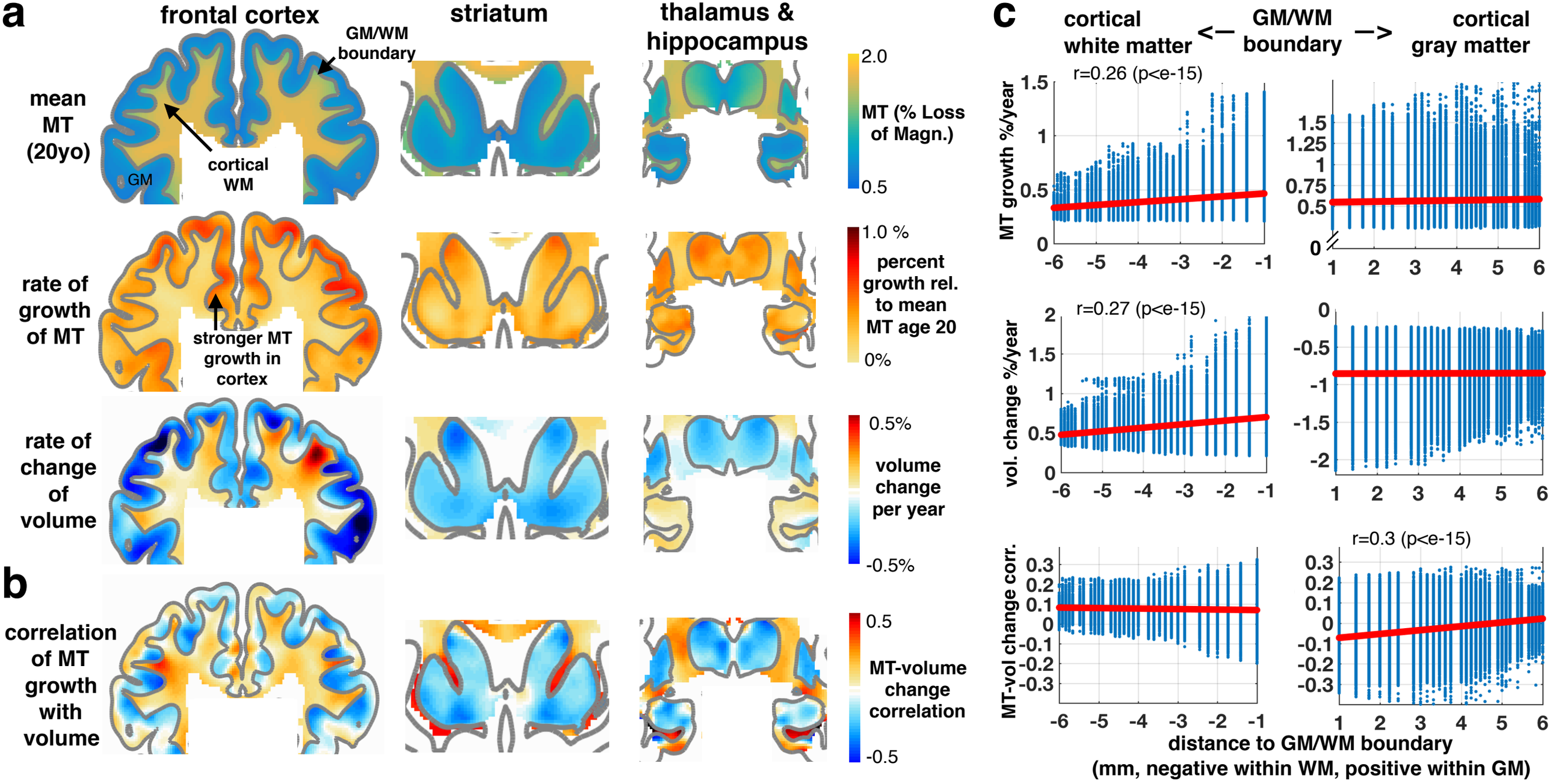
a
frontal cortex
striatum
thalamus & hippocampus
GM/WM boundary
mean MT (20yo)
GM
cortical WM
rate of growth of MT
stronger MT growth in cortex
rate of change of volume
b
correlation of MT growth with volume
2.0
MT (% Loss of Magn.)
0.5
1.0 %
percent growth rel. to mean MT age 20
0%
0.5%
volume change per year
-0.5%
0.5
MT-volume change correlation
-0.5
c
cortical white matter
<—
GM/WM boundary
—>
cortical gray matter
r=0.26 (p<e-15)
MT growth %/year
r=0.27 (p<e-15)
vol. change %/year
r=0.3 (p<e-15)
MT-vol change corr.
distance to GM/WM boundary
(mm, negative within WM, positive within GM)

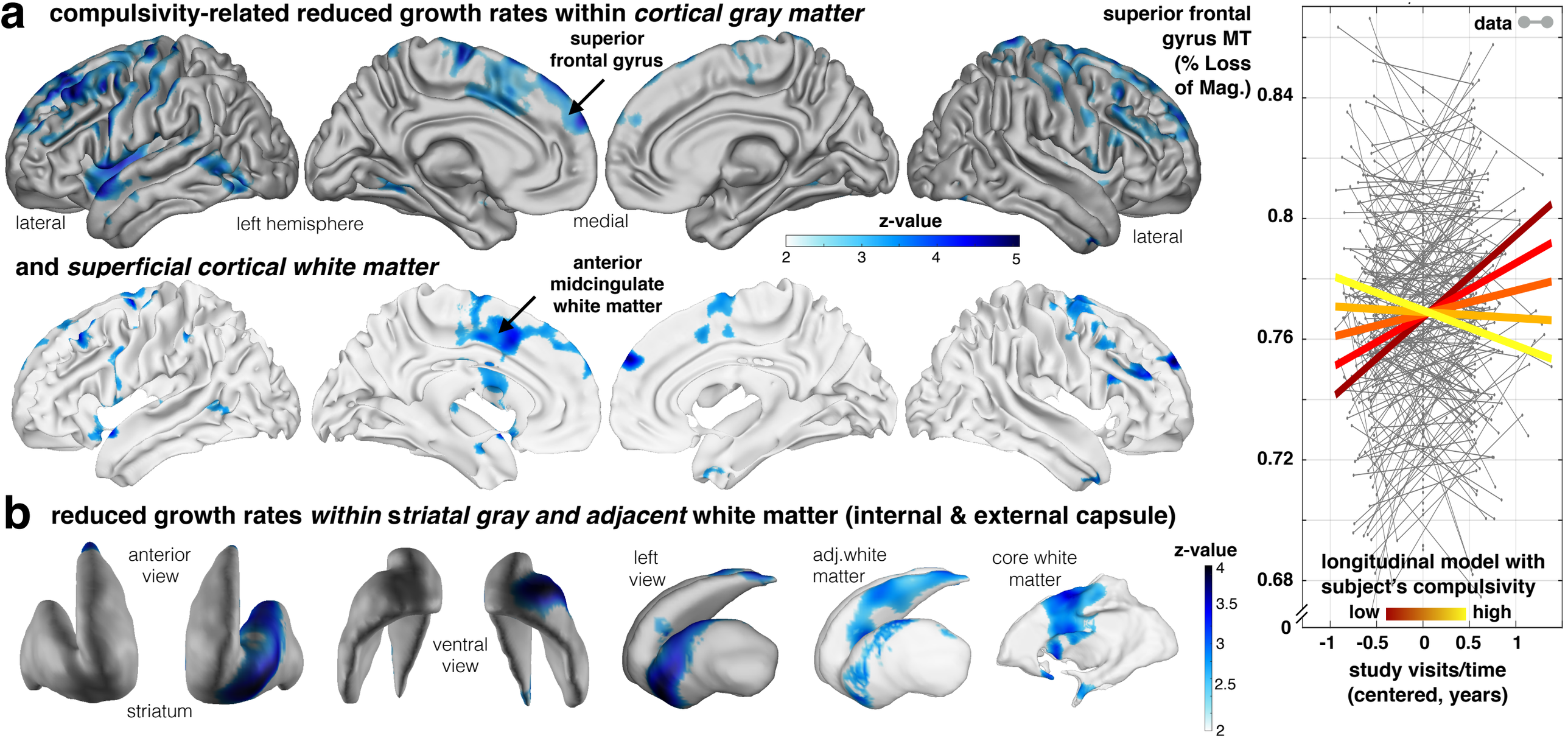
a
compulsivity-related reduced growth rates within cortical gray matter
superior frontal gyrus
lateral
left hemisphere
medial
lateral
z-value
2
3
4
5
and superficial cortical white matter
anterior midcingulate white matter
b
reduced growth rates within striatal gray and adjacent white matter (internal & external capsule)
anterior view
striatum
ventral view
left view
adj.white matter
core white matter
z-value
4
3.5
3
2.5
2
superior frontal gyrus MT (% Loss of Mag.)
data
0.84
0.8
0.76
0.72
0.68
0
longitudinal model with subject's compulsivity
low
high
-1
-0.5
0
0.5
1
study visits/time (centered, years)

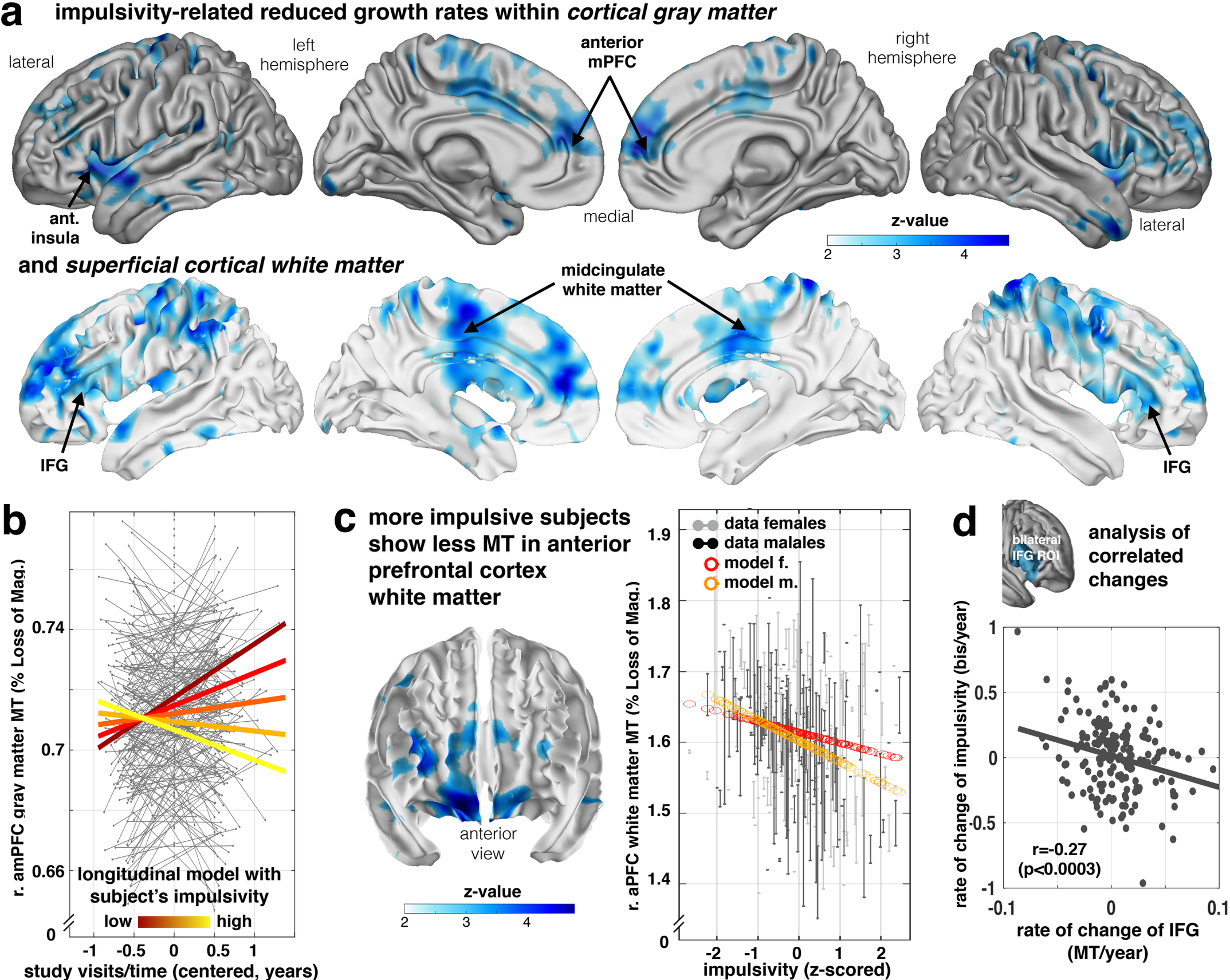
a
impulsivity-related reduced growth rates within cortical gray matter
lateral
left hemisphere
anterior mPFC
right hemisphere
ant. insula
medial
lateral
z-value
2
3
4
and superficial cortical white matter
midcingulate white matter
IFG
IFG
b
r. amPFC gray matter MT (% Loss of Mag.)
0.74
0.7
0.66
0
longitudinal model with subject's impulsivity
low
high
-1
-0.5
0
0.5
1
study visits/time (centered, years)
c
more impulsive subjects show less MT in anterior prefrontal cortex white matter
anterior view
z-value
2
3
4
data females
data malales
model f.
model m.
r. aPFC white matter MT (% Loss of Mag.)
1.9
1.8
1.7
1.6
1.5
1.4
0
-2
-1
0
1
2
impulsivity (z-scored)
d
bilateral IFG ROI
analysis of correlated changes
rate of change of impulsivity (bis/year)
1
0.5
0
-0.5
-1
r=-0.27
(p<0.0003)
-0.1
0
0.1
rate of change of IFG (MT/year)